Characterization of the Bonding Zone in a ZE41/AlSi12 Joint Fabricated by Liquid-Solid Compound Casting

R. Mola, T. Bucki *
Kielce University of Technology
al. Tysiąclecia Państwa Polskiego 7, 25-314 Kielce, Poland
* Corresponding author. E-mail address: tbucki@tu.kielce.pl

Abstract

The study involved using the liquid-solid compound casting process to fabricate a lightweight ZE41/AlSi12 bimetallic material. ZE41 melt heated to 660 ºC was poured onto a solid AlSi12 insert placed in a steel mold. The mold with the insert inside was preheated to 300 ºC. The microstructure of the bonding zone between the alloys was examined using optical microscopy and scanning electron microscopy. The chemical composition was determined through linear and point analyses with an energy-dispersive X-ray spectroscope (EDS). The bonding zone between the magnesium and aluminum alloys was about 250 μm thick. The results indicate that the microstructure of the bonding zone changes throughout its thickness. The structural constituents of the bonding zone are: a thin layer of a solid solution of Al and Zn in Mg and particles of Mg-Zn-RE intermetallic phases (adjacent to the ZE41 alloy), a eutectic region ($Mg_{17}(Al,Zn)_{12}$ intermetallic phase and a solid solution of Al and Zn in Mg), a thin region containing fine, white particles, probably Al-RE intermetallic phases, a region with Mg_2Si particles distributed over the eutectic matrix, and a region with Mg_2Si particles distributed over the Mg-Al intermetallic phases matrix (adjacent to the AlSi12 alloy). The microstructural analysis performed in the length direction reveals that, for the process parameters tested, the bonding zone forming between the alloys was continuous. Low porosity was observed locally near the ZE41 alloy. The shear strength of the AZ91/AlSi17 joint varied from 51.3 to 56.1 MPa.

Keywords: Innovative Foundry Technologies and Materials, Compound Casting Process, Magnesium Alloy, Aluminum Alloy, Bonding Zone

1. Introduction

Compound casting is a method employed to produce bimetal parts. In recent years, much research has been conducted to use this casting method to join different metallic materials, for instance, various Fe alloys [1-3], steel to Al alloys [4-5], Al to Cu [6], various Al alloys [7-9], and various Mg alloys [10]. This method has been applied also to produce bimetal Mg-Al elements. Magnesium alloys have lower density than aluminum alloys (1.4-

1.9 Mg/m^3 and about 2.7 Mg/m^3, respectively); magnesium alloys are also characterized by higher relative strength and much better machinability. Some of the properties of magnesium alloys, however, are definitely inferior to those of aluminum alloys; these are low tensile strength at elevated temperatures, low creep strength and reduced plastic deformability at room temperature. When compared with aluminum alloys, magnesium alloys also have lower impact resistance as well as much lower resistance to corrosion and abrasion [11]. Thus, when the two light alloys are joined together, it is possible to obtain an attractive bimetallic

material with properties superior to those of single body Mg-based or Al-based material. The Mg-Al bimetal seems to have many potential applications, for example, in the transport industry. Compared to other joining techniques, compound casting enables production of Mg-Al bimetal parts of any shape and dimension.

The literature dealing with the use of compound casting to produce Mg-Al bimetals discusses the joining of pure Mg to pure Al [12-16], pure Mg to AlMg1 aluminum alloy [7], AZ91 magnesium alloy to A356 aluminum alloy [17] and AZ91 magnesium alloy to AlSi17 aluminum alloy [18-20]. As shown above, most studies have been concerned with pure Mg and pure Al. In such a case, the bonding zone consists of the following phases: a solid solution of Al in Mg, an Al_3Mg_2 intermetallic phase, an $Mg_{17}Al_{12}$ intermetallic phase and a solid solution of Mg in Al. Since pure Mg and pure Al are rarely applied as structural materials, it is vital that more intensive research be undertaken on the use of compound casting to join different magnesium alloys to different aluminum alloys. A high concentration of additional alloying elements in the alloys joined may lead to considerable changes in the bonding zone structure. In their earlier studies [18-20], the authors discuss the results concerning the bonding of AZ91 magnesium alloy with AlSi17 aluminum alloy by compound casting. The bonding zone forming between the two alloys had a multiphase structure. In the area close to the AZ91 magnesium alloy, a eutectic (an $Mg_{17}Al_{12}$ intermetallic phase + a solid solution of Al and in Mg) was observed. At a certain distance from the AZ91 alloy, an Mg_2Si phase co-occurred with the eutectic. In the area adjacent to the AlSi17 aluminum alloy, fine Mg_2Si particles over the Mg-Al intermetallic phases matrix were reported.

In this study, the liquid-solid compound casting process was used to join ZE41 magnesium alloy to AlSi12 aluminum alloy. Liquid ZE41 was poured onto a solid AlSi12 alloy insert placed in the mold. The article focuses on the microstructural analysis of the bonding zone.

2. Experimental procedure

ZE41 magnesium alloy and AlSi12 aluminum alloy were used as the cast material and the insert material, respectively. The compositions of the alloys used in this study are given in Table 1.

Table 1.
Chemical compositions (wt.%) of the alloys bonded

Alloy	Mg	Al	Zn	Si	Mn	Zr	Fe	Cu
ZE41	bal.	-	4.0	-	0.01	0.52	-	-
Total Rare Earth (TR) = 1.3, Ce-to-TR ratio (Ce/TR) = 50								
AlSi12	0.15	bal.	0.01	10.97	0.43	-	0.26	0.15

Cylindrical inserts, 30 mm in diameter and 10 mm in thickness, were cut from rapidly solidified AlSi12 alloy. The surface of the insert was ground with silicon carbide papers up to 800 grit and then cleaned with ethanol. Then, the insert was placed at the bottom of a steel mold. The mold with an insert inside was pre-heated up to about 300 °C. 100 g of ZE41 alloy was melted under pure argon atmosphere and then poured at 660 °C onto the AlSi12 insert placed in the mold.

The cylindrical ZE41/AlSi12 bimetal samples fabricated by compound casting were cut along the central axis. The samples were prepared for microscopic observations following standard metallographic procedures. The final polishing was performed using 0.05 μm colloidal silica. The samples were not etched. The microstructure of the bonding zone was examined over the entire cross-section. The microstructural investigations were conducted with a Nikon ECLIPSE MA 200 optical microscope and a JEOL JSM-5400 scanning electron microscope. The compositions of the particular phases reported in the bonding zone were determined using an energy dispersive X-ray spectroscope (EDS) detector that the SEM microscope was fitted with.

The strength of the bonding zone of the ZE41/AlSi12 bimetal samples was assessed through shear strength tests performed with a LabTest5.20SP1 universal testing machine at a displacement of 10 mm/min. As pure shear is a stress state that is difficult to achieve, simple shear tests were carried out. A schematic diagram of the simple shear test setup is illustrated in Fig. 1 [20].
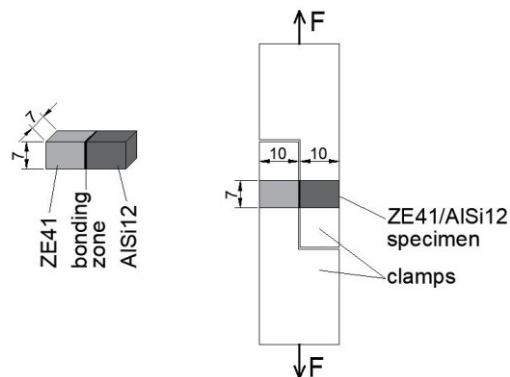

Fig. 1. Schematic diagram of the shear strength test

3. Results and discussion

Figure 2(a) presents a low magnification optical microscopic image of a bimetallic ZE41/AlSi12 sample produced by liquid-solid compound casting. The bonding zone between the magnesium alloy and the aluminum alloy had a thickness of about 250 μm. The high magnification images in Figs. 2(b), 2(c) and 2(d) show the microstructure of the bonding zone in the area close to the ZE41, in the central area and in the area close to the AlSi12 alloy, respectively. As can be seen, the microstructure of the bonding zone changes throughout its thickness from the magnesium alloy to the aluminum alloy. In the upper part of Fig. 2(b), the microstructure of the ZE41 alloy is visible. Particles of the dark phase are located at the boundaries of and inside the grains of the solid solution of Zn in Mg. The microstructure of the AlSi12 alloy insert after thermal modification can be seen at the bottom of Fig. 2(d). The structure is characterized by dendrites of the α-Al and fine eutectic in the interdendritic areas.
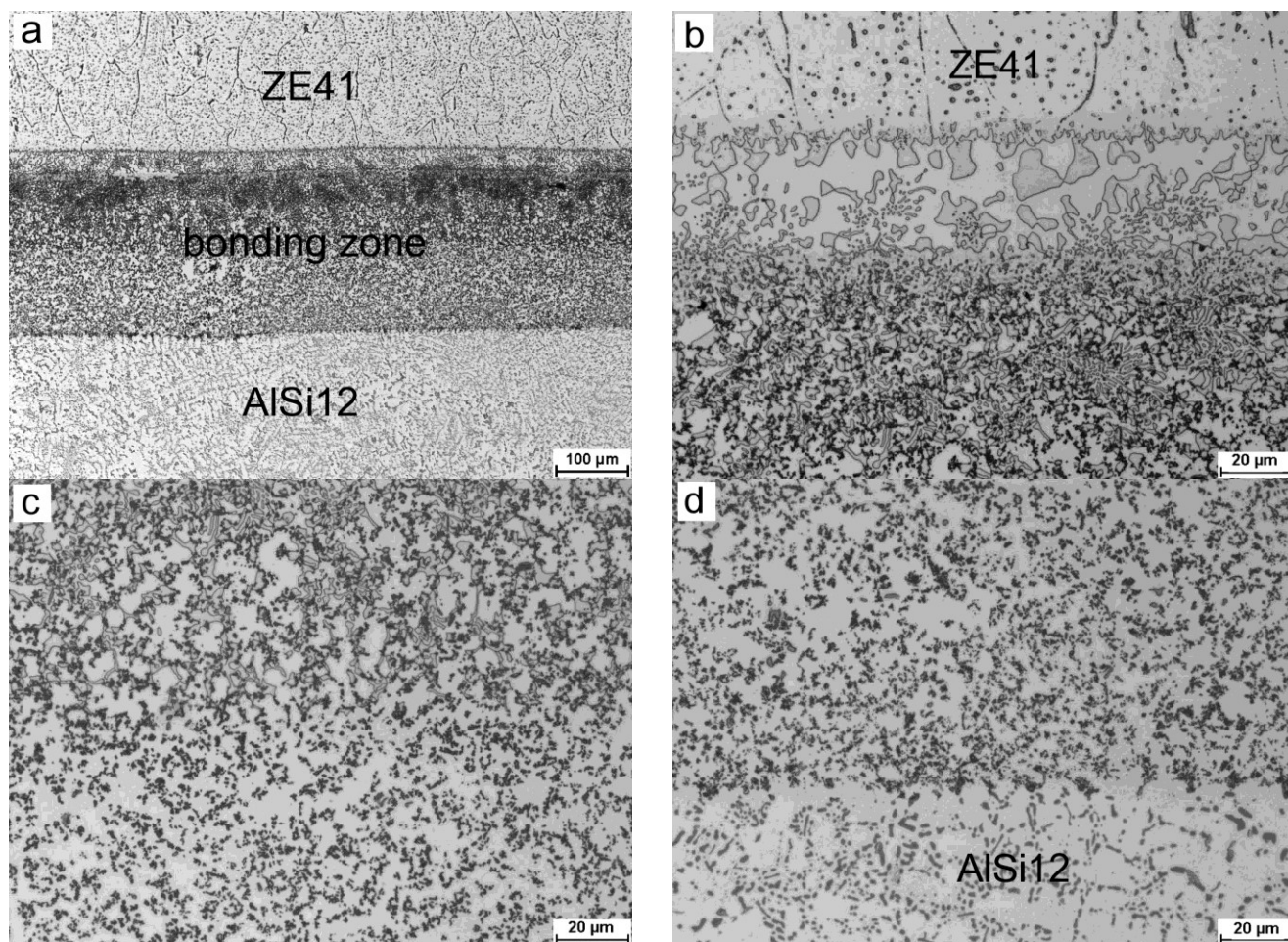
Fig. 2. OM images of the microstructure of the bonding zone in the bimetallic ZE41/AlSi11 sample produced by liquid-solid compound casting; (a) low magnification, (b-d) high magnification: (b) area close to the ZE41, (c) central area, (d) area close to the AlSi12 alloy

An SEM analysis of the bonding zone was carried out to determine further details. Figure 3 shows the microstructure of the zone on the ZE41 alloy side with marked points of the quantitative EDS analysis and the corresponding line scan results. Table 2 presents the EDS data. The quantitative analysis of the ZE41 alloy matrix (points 1 and 2) indicates the presence of a solid solution of Zn in Mg. Some examinations revealed a small amount of Zr in these areas (point 2). The elemental analysis of the particles observed at the boundaries of and inside the grains (points 3 and 4) indicates that they are rich in Mg, Zn, La, Ce and Nd. The results are in agreement with the literature data [21-23]; they show that the structure of the ZE41 alloy consists of α-Mg grains and an Mg-Zn-RE intermetallic phase (with a wide range of composition) at the grain boundaries. Al was detected in the ~10 μm thick darker region of the ZE41 alloy adjacent to the bonding zone (points 5 and 6). The linear and point analyses show that the concentration of Al in this region increases with increasing distance from the ZE41. As mentioned above, the quantitative analysis of the ZE41 matrix outside the darker region did not reveal the occurrence of Al. This indicates that the solid solution of Al and Zn in Mg and the particles of the Mg-Zn-RE intermetallic phase are the first structural constituents of the

bonding zone detected on the ZE41 alloy side. Next, there is a two-phase area composed of the darker and lighter phases. According to the Al-Mg-Zn phase diagram [24], the chemical composition of the lighter phase (point 7) corresponds to that of the $Mg_{17}(Al,Zn)_{12}$ intermetallic phase. The composition of the darker phase (point 8) is similar to that of the solid solution of Al and Zn in Mg. The results suggest that the two-phase structure is a eutectic composed of $Mg_{17}(Al,Zn)_{12}$ and a solid solution of Al and Zn in Mg. Close to the eutectic, there is a region with fine, white particles. The EDS line scan results indicate a high concentration of rare earth elements (Ce, Nd and La) and Zr in this area. The white particles were too small in size to assess their chemical composition with the test analysis used (EDS point analysis). The quantitative analysis (point 9) confirmed the presence of the rare earth elements and Zr in this region. A high content of Al was also detected. According to the literature data, these fine, white particles are probably the Al-RE intermetallic phases [25]. As can be seen from the line scan results in Fig. 3, the concentration of Mg, Al and Si in the next region (adjacent to the white-particle region) was high. The microstructure of this region examined through optical microscopy can be seen at the bottom of Fig. 3(b). Numerous fine, dark particles are visible over the eutectic

structure. The high concentration of Si in this region indicates that the dark particles co-occurring with the eutectic are rich in Si.
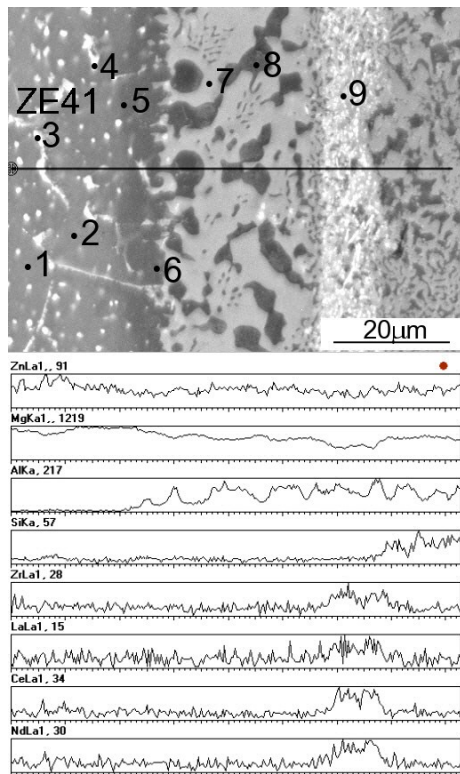

Fig. 3. SEM image of the bonding zone observed on the ZE41 alloy side with a distribution of elements along the marked line

Table 2.
Results of the EDS quantitative analysis at points marked in Fig. 3

Point	Mg	Al	Zn	Si	Zr	La	Ce	Nd
				% at.				
1	98.84	-	1.16	-	-	-	-	-
2	98.70	-	1.18	-	0.12	-	-	-
3	92.51	-	6.25	-	-	0.42	0.68	0.14
4	91.07	-	7.68	-	-	0.33	0.67	0.25
5	98.13	0.67	1.20	-	-	-	-	-
6	92.59	6.66	0.75	-	-	-	-	-
7	62.20	34.93	2.87	-	-	-	-	-
8	82.80	16.31	0.89	-	-	-	-	-
9	57.42	36.85	2.10	0.38	1.18	0.59	1.06	0.42

The microstructure of the central area of the bonding zone is presented in Fig. 4. The distribution of the elements along the marked line indicates that the fine, dark particles rich in Si are present in the entire central area of the bonding zone. It can be seen that the microstructure of the central area on the ZE41 alloy side (left part of the image) differs from that on the AlSi12 side (right part of the image). The eutectic structure observed on the ZE41 alloy side diminishes. On the AlSi12 alloy side, Si-rich particles are detected over the light phase matrix. In the SEM image (Fig. 4), the Si rich particles are as dark as the solid solution and they are located mainly close to the solid solution; it is thus difficult to distinguish between the two constituents of the

microstructure. The EDS analysis of the white area of the eutectic structure (point 1: 64.17 at. % Mg, 33.92 at. % Al, 1.91 at. % Zn) confirms the occurrence of the $Mg_{17}(Al,Zn)_{12}$ intermetallic phase. The chemical composition of the light phase matrix (point 2: 62.73 at. % Mg, 36.91 at. % Al, 0.36 at. % Zn) corresponds also to the $Mg_{17}(Al,Zn)_{12}$ intermetallic phase. The microstructure of the central area of the bonding zone contains white particles as well. The distribution of the elements along the marked line indicates that the particles are rich in Al, Si, Mn and Fe. The AlSi12 alloy contains small amounts of Mn and Fe. Hence the presence of the multicomponent phase in the bonding zone.
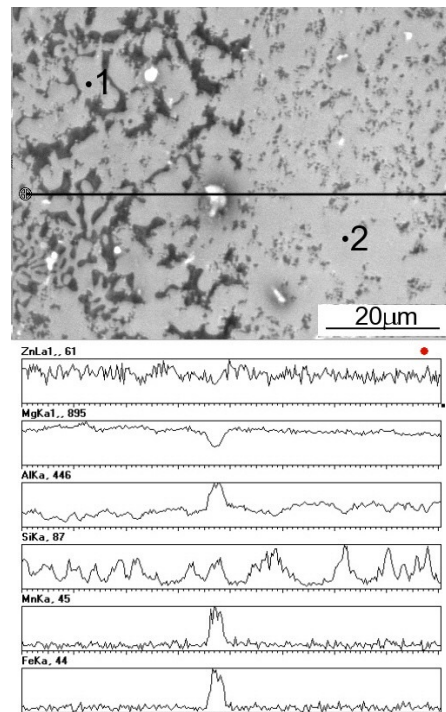

Fig. 4. SEM image of the central area of the bonding zone with a distribution of elements along the marked line

Figure 5 shows details of the microstructure of the bonding zone close the AlSi12 alloy. Fine, dark particles are visible over the light phase matrix. Locally, these particles form agglomerates. The EDS quantitative analysis was performed in the dark particle agglomerates (point 1: 68.12 at. % Mg, 31.18 at. % Si, 0.7 at. % Al). The Mg:Si ratio corresponding to the 2:1 stoichiometry for Mg_2Si what suggests that the dark particles are the Mg_2Si phase. The concentration of Al in the light matrix (point 2: 40.13 at. % Mg, 57.43 at. % Al, 2.44 at. % Si) is higher than that observed in the light matrix in the central area of the bonding zone. This suggests that the Al_3Mg_2 intermetallic phase close to the AlSi12 alloy richer in Al than the $Mg_{17}Al_{12}$ is the matrix of the bonding zone. In their previous works [18-20] concerning the fabrication of AZ91/AlSi17 joints by compound casting, the authors showed that the Mg_2Si phase and the Al_3Mg_2 intermetallic phase were the structural constituents of the bonding zone on the Al-Si alloy side. As can be seen from Fig. 5, the white particles rich in Al, Si, Mn and Fe are present both in the AlSi12 alloy and the bonding zone.
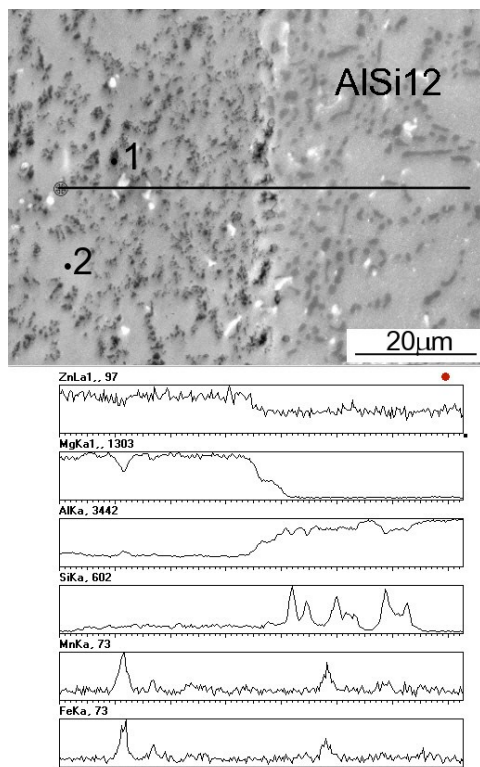
Fig. 5. SEM image of the bonding zone observed on the AlSi12 alloy side with a distribution of elements along the marked line

Fig. 6. Optical micrograph of the ZE41/AlSi12 bimetallic sample fabricated by compound casting with some porosity visible in the bonding zone

From the microstructural analysis of the bonding zone of the ZE41/AlSi12 bimetallic sample in the length direction it is evident that the zone obtained at the selected process parameters was continuous. Locally small porosity was observed (Fig. 6). Pores were visible in the region close to the ZE41 alloy, where the main structural constituent of the bonding zone was the eutectic.

The shear strength of the bonding zone in the ZE41/AlSi12 bimetallic samples ranged from 51.3 to 56.1 MPa. Figure 7 shows a fractured sample. The horizontal crack propagates towards the bonding zone. As can be seen, the microstructure of the bonding zone changes throughout its thickness; several zones can be distinguished. The crack does not run through one zone only; it jumps between zones. This suggests similar strength of the zones. The brittle fracture indicates that the bonding zone is composed of hard, brittle intermetallic phases responsible for relatively poor mechanical properties of the joint. As suggested by the literature data [15], the shear strength of the Mg/Al bimetal depends on the thickness of the bonding zone. The decrease in the shear strength of the bonding zone in the Mg/Al bimetal was due to an increase in its thickness. The properties of the ZE41/AlSi12 joint could be improved by modifying the structure of the bonding zone through reducing its thickness, which could be achieved by using appropriate process parameters.
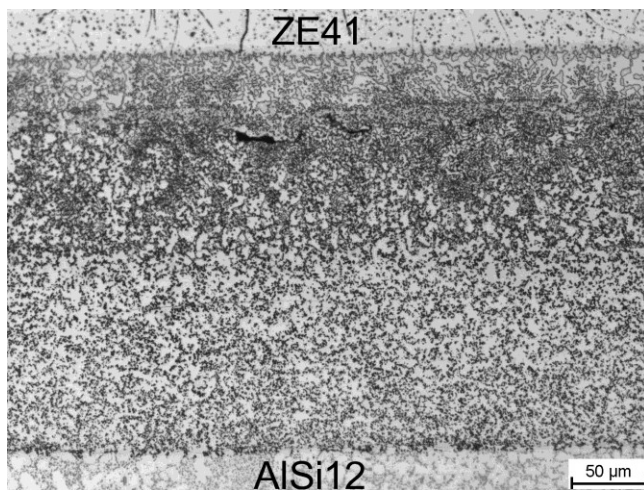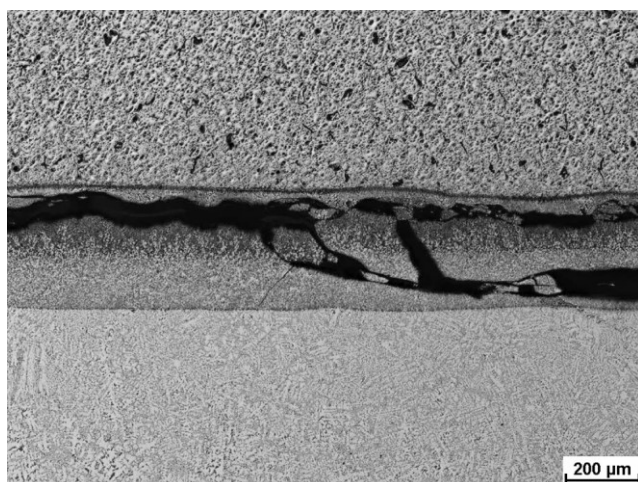

Fig. 7. Shear-fractured bonding zone of the ZE41/AlSi12 bimetallic specimen

4. Conclusions

The microstructure of the bonding zone was analyzed using an optical microscope and a scanning electron microscope equipped with an energy dispersive spectroscope (EDS). The following conclusions can be drawn:
1. The bimetallic joint was obtained by pouring liquid ZE41 magnesium alloy (660 ºC) onto a solid AlSi12 aluminum alloy insert placed in a mold (both preheated to 300 ºC).
2. The optical microscopic examinations of the ZE41/ASi12 bimetallic sample reveal that a continuous bonding zone with a thickness of about 250 μm formed between the alloys. Low porosity was observed locally near the ZE41 alloy, where the main structural constituent of the bonding zone was the eutectic.

3. The microstructure of the bonding zone was non-homogenous; it changed throughout its thickness.
4. The detailed SEM analysis shows that the structural constituents of the bonding zone are: a thin region of a solid solution of Al and Zn in Mg and particles of the Mg-Zn-RE intermetallic phase (adjacent to the ZE41 alloy), a eutectic region with an $Mg_{17}(Al,Zn)_{12}$ intermetallic phase and a solid solution of Al and Zn in Mg, a thin region containing fine, white particles, most probably of the Al-RE intermetallic phases, a region with Mg_2Si particles distributed over the eutectic matrix, and a region with Mg_2Si particles distributed over the Mg-Al intermetallic phase matrix (adjacent to the AlSi12 alloy).
5. The shear strength of the ZE41/ASi12 bimetallic samples varied between 51.3 and 56.1 MPa.

References

[1] Avci, A., Ilkaya, N., Simsir, M.M. & Akdemir, A. (2009). Mechanical and microstructural properties of low-carbon steel-plate-reinforced gray cast iron. *Journal of Materials Processing Technology.* 209(3), 1410-1416.

[2] Wróbel, T. (2014). Characterization of bimetallic castings with an austenitic working surface layer and an unalloyed cast steel base. *Journal of Materials Engineering and Performance.* 23(5), 1711-1717.

[3] Wróbel, T. & Szajnar, J. (2015). Bimetallic casting: ferritic stainless steel-grey cast iron. Archives of Metallurgy and Materials. 60(3), 2361-2365.

[4] Choe, K.H., Park, K.S., Kang, B.H., Cho, G.S., Kim, K.Y., Lee, K.W., Kim, M.H., Ikenaga, A. & Koroyasu, S. (2008). Study of the interface between steel insert and aluminum casting in EPC. *Journal of Materials Science & Technology.* 24, 60-64.

[5] Szymczak, T. (2011). The influence of selected technological factors on the quality of bimetallic castings alloy steel-silumin. *Archives of Foundry Engineering.* 11(3), 215-226.

[6] Zare, G.R., Divandari, M. & Arabi, H. (2013). Investigation on interface of Al/Cu couples in compound casting. *Materials Science and Technology.* 29, 190-196.

[7] Papis, K.J.M., Loeffler, J.F. & Uggowitzer, P.J. (2009). Light metal compound casting. *Science in China Series E: Technological Sciences.* 52(1), 46-51.

[8] Papis, K.J.M., Hallstedt, B., Löffler, J.F. & Uggowitzer, P.J. (2008). Interface formation in aluminium - aluminium compound casting. *Acta Materialia.* 56, 3036-3043.

[9] Sun, J., Song, X., Wang, T., Yu, Y., Sun, M., Cao, Z. & Li, T. (2012). The microstructure and property of Al-Si alloy and Al-Mn alloy bimetal prepared by continuous casting. *Materials Letters.* 67, 21-23.

[10] Papis, K.J.M., Löffler, J.F. & Uggowitzer, P.J. (2010). Interface formation between liquid and solid Mg alloys - an approach to continuously metallurgic joining of magnesium parts. *Materials Science and Engineering. A* 527, 2274-2279.

[11] Dziadoń, A. & Mola, R. (2013). Magnesium – trends of development of mechanical properties. *Obróbka plastyczna metali.* 24(4), 253-277.

[12] Paramsothy, M., Srikanth, N. & Gupta, M. (2008). Solidification processed Mg/Al bimetal macrocomposite: Microstructure and mechanical properties. *Journal of Alloys and Compound.* 461, 200-208.

[13] Hajjari, E., Divandari, M., Razavi, S.H., Emami, S.M., Homma, T. & Kamado, S. (2011). Dissimilar joining of Al/Mg light metals by compound casting process. *Journal of Materials Science.* 46, 6491-6499.

[14] Hajjari, E., Divandari, M., Razavi, S.H., Homma, T. & Kamado, S. (2012). Intermetallic compounds and antiphase domains in Al/Mg compound casting. *Intermetallics.* 23, 182-186.

[15] Emami, S.M., Divandari, M., Arabi, H. & Hajjari, E. (2013). Effect of melt-to-solid insert volume ratio on Mg/Al dissimilar metals bonding. *Journal of Materials Engineering and Performance.* 22(1), 123-130.

[16] Mola, R., Bucki, T. & Dziadoń, A. (2016). Formation of Al-alloyed layer on magnesium with use of casting techniques. *Archives of Foundry Engineering.* 16(1), 112-116.

[17] Li, G., Jiang, W., Fan, Z., Jiang, Z. & Liu, X. (2016). Effects of pouring temperature on microstructure, mechanical properties, and fracture behavior of Al/Mg bimetallic composites produced by lost foam casting process. *The International Journal of Advanced Manufacturing Technology.* 91(1-4), 1355-1368.

[18] Mola, R., Bucki, T. & Dziadoń, A. (2017). Effects of the pouring temperature on the formation of the bonding zone between AZ91 and AlSi17 in the compound casting process. *IOP Conference Series: Materials Science and Engineering.* 179(1), 1-6.

[19] Mola, R., Bucki, T. & Dziadoń, A. (2017). Microstructure of the bonding zone between AZ91 and AlSi17 formed by compound casting. *Archives of Foundry Engineering.* 17(1), 202-206.

[20] Mola, R. & Bucki, T. (2018). The microstructure and properties of the bimetallic AZ91/AlSi17 joint produced by compound casting. *Archives of Foundry Engineering.* 18(1), 71-76.

[21] Wei, L.Y., Dunlop, G.L. & Westengen, H. (1995). Percipitation hardening of Mg-Zn and Mg-Zn-RE alloys. *Metallurgical and Materials Transactions.* A 26, 1705-1716.

[22] Huang, M.L., Li, H.X., Ding, H., Ren, Y.P., Qin, G.W. & Hao, S.M. (2009). Partial phase relationship of Mg-Zn-Ce system at 350ºC. *The Transactions of Nonferrous Metals Society of China.* 19, 681-685.

[23] Neil, W.C., Forsyth, M., Howlett, P.C., Hutchinson, C.R. & Hinton, B.R.W. (2011). Corrosion of heat treated magnesium alloy ZE41. Corrosion *Science.* 53(10), 3299-3308.

[24] Ohno, M., Mirkovic, D. & Schmid-Fetzer, R. (2006) Phase equilibria and solidification of Mg-rich Mg-Al-Zn alloys. *Materials Science and Engineering. A* 421, 328-337.

[25] Chaubey, A.K., Scudino, S., Prashanth, K.G. & Eckert, J. (2015). Microstructure and mechanical properties of Mg-Al-based alloy modified with cerium. *Materials Science and Engineering. A* 625, 46-49.